Progress In Electromagnetics Research C, Vol. 121, 145–161, 2022

Modeling Dipole Arrays that Produce Synthesized Patterns Using NEC

Edmund K. Miller*

Abstract—Pattern synthesis usually involves determining the strengths of the currents in a given array so that it radiates a specified pattern. Demonstrating that this pattern can be produced by an actual array of physical elements is the next step in the synthesis problem. This entails determining the excitations needed for a physical array when mutual interactions are accounted for. These excitations can be either source voltages or the synthesized currents themselves, with both options available in NEC 4 (the Numerical Electromagnetics Code). While this is done here using NEC, the same approach could use any wire-antenna computer code. When the current option is chosen, the code first solves for the voltages that induce the required currents. This is a simple procedure that automatically includes the effect of mutual coupling among the array elements. The purpose of this article is to examine how well a numerical model of a given array will match the specified pattern. Several examples of this approach are included here to demonstrate the process.

1. INTRODUCTION

The pattern-synthesis problem involves determining the complex (possibly) values of the N current elements required to produce a desired radiation pattern from a specified array configuration using various analytical procedures [1–19]. The next step is to then design a physical antenna of N wire dipoles of appropriate lengths and radii and excited so as to carry the currents derived in the synthesis process. The most critical part of this step is determining the exciting voltages needed to induce the needed current values in the physical array while including the interaction effects among the antenna elements.

The Numerical Electromagnetics Code (NEC) includes two options for exciting a wire structure being modeled as an antenna. The more-often used option is to specify the input voltage(s) that excites it. An alternative option is to instead specify the input current(s), the approach used here for the synthesis problem, a feature offered in NEC version 4.2. It is worth emphasizing that this approach is compatible with any numerical antenna-array model. Unless stated otherwise, the NEC-array models used for the results that follow consist of 7-segment, half-wavelength dipoles 10^{-3} wavelengths in radius. The dipoles are parallel to the z-axis with their centers at $z = 0$ as illustrated below and the patterns are computed in the X-Y plane. The dipoles are equally spaced along the x-axis except for 3.2 where they are randomly located, and 3.3 and 3.4 where the array elements lie in the x-y plane.

Observe that this discussion is not about pattern-synthesis methodology *per se* but instead addresses the question about whether a real antenna, i.e., one that is modeled numerically using a validated computer code, will radiate the pattern of interest. For those who might want to investigate various pattern synthesis approaches, a representative list of relevant articles is included in [1–19]. A reviewer observed "the problem of synthesized arrays by actual antenna has already been discussed by many papers" and provided 3 examples. Of the 3 only one of these [20] is relevant but the approach

Received 12 May 2022, Accepted 24 June 2022, Scheduled 14 July 2022
* Corresponding author: Edmund K. Miller (e.miller@ieee.org).
The author is with the Los Alamos National Laboratory (Retired), USA.

it presents for including mutual coupling requires 3 journal pages to describe. This is much more complicated than that offered by the NEC approach which uses only the synthesized currents as the input to the NEC model. A thorough review of the mutual-coupling problem can be found in [21]. The combination of the synthesis procedure in [22] with the current-input treatment included in NEC offers a straightforward way to synthesize non-uniform and non-linear geometries.

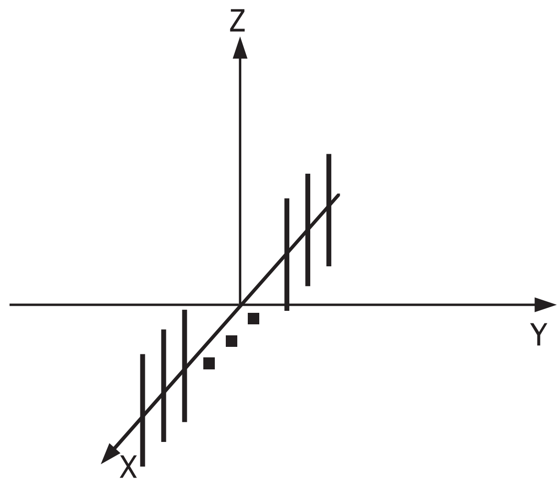

Array with equally spaced elements aligned along the X axis.

2. REPRESENTATIVE NUMERICAL RESULTS

In a previous article [20] a synthesis procedure was described for creating a variety of patterns based on iteratively deriving the element currents of a prescribed array that produce a specified sequence of associated pattern maxima. This iterative approach was demonstrated to converge to the desired pattern maxima for arrays having equal sidelobe levels such as the Dolph-Chebyshev array and various other sidelobe specifications, usually in fewer than a dozen iterations. The synthesis approach in [20] was demonstrated to provide results that conformed to a variety of specified patterns, some of which are examined here to test their compatibility with an actual physical array. Another procedure for synthesizing the element locations and currents based on Prony's Method was described in [23]. An example developed from that approach is also included.

The pattern-synthesis results included in the following were obtained with 24-digit compute precision using Future Basic, a compiled language for Macintosh computers. The NEC computations were done using a Fortran version for the HP computer and performed in double precision. Note that the dipole excitation voltages are specific to the tangential-electric-field source model used in NEC.

Upon running NEC using the currents determined for some of the synthesized patterns and arrays discussed in [20], the excitation voltages for the array dipoles are obtained as are their associated patterns. The NEC-derived patterns and the original synthesized patterns from [20] are then plotted together to determine how closely the physical (NEC-modeled) array pattern agreed with them. The NEC excitation voltages are listed only for the first two examples since their specific values can depend somewhat on the source treatment used for a numerical model. The element currents are included for all of the examples for readers to perform similar experiments using their own models.

3. DOLPH-CHEBYSHEV PATTERNS

3.1. The Standard Dolph-Chebyshev Array

The pattern of a Dolph-Chebyshev (DC) array is one of the more popular examples of pattern synthesis. The patterns included in Fig. 1 are for a 4-wavelength, 9-element array with -20 dB sidelobes. The

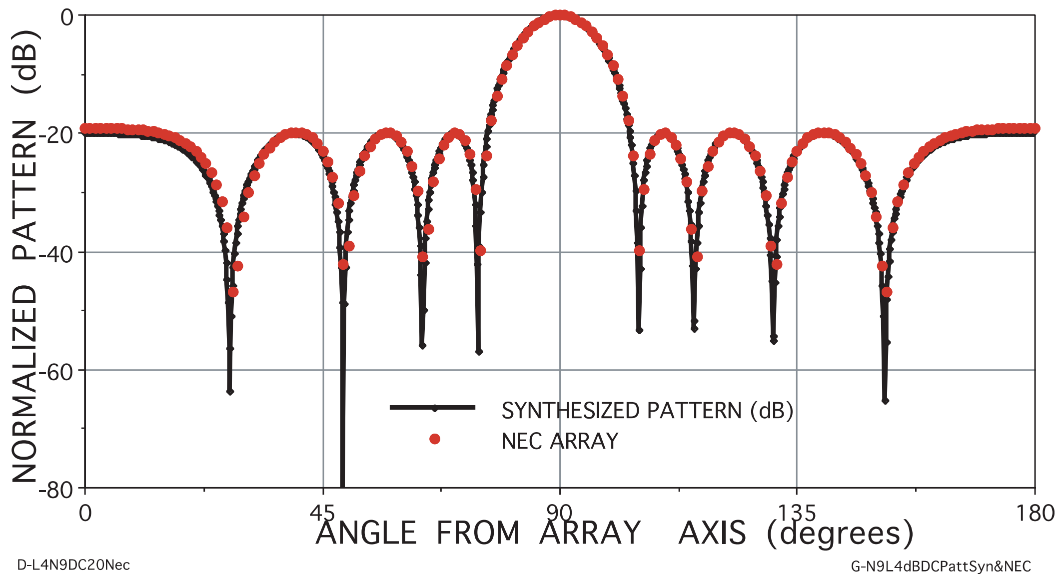

Figure 1. The synthesized and NEC-computed patterns for a 9-element, 4-wavelength DC array with −20 dB sidelobes.

pattern from the NEC model agrees to within a few tenths of a dB with the DC array of specified element currents except for the widest sidelobe where the difference is 0.76 dB. For reference purposes, the DC currents derived for the synthesized pattern and the excitation voltages needed for the NEC array are included in Table 1 for the DC array and in Table 2 for the randomized DC array. Tables 3–11 for the remaining 9 arrays include only the array currents.

Table 1. Exciting voltages and currents for the 9-element Dolph-Chebyshev array having −20 dB sidelobes of Fig. 1.

Element No.	V Real	V Imag	I Real	I Imag
1	7.20977E+1	3.21162E+1	1E+0	0E+0
2	4.99843E+1	−1.38425E+1	1.0231E+0	0E+0
3	8.32325E+1	2.38433E+1	1.3501E+0	0E+0
4	8.80578E+1	−2.71995E+0	1.5796E+0	0E+0
5	1.00128E+2	2.34736E+1	1.6622E+0	0E+0
6	8.80578E+1	−2.71995E+0	1.5796E+0	0E+0
7	8.32325E+1	2.38433E+1	1.3501E+0	0E+0
8	4.99843E+1	−1.38425E+1	1.0231E+0	0E+0
9	7.20977E+1	3.21162E+1	1E+0	0E+0

3.2. A Randomized Dolph-Chebyshev Array

The next variation on the −20 dB DC array is for a linear array 3.62 wavelengths long having randomly spaced dipoles along the x-axis as depicted in Fig. 3(a). The radiation pattern (b) exhibits agreement with the intended pattern somewhat similar to that of Fig. 1 for the end lobes but with more variation in the interior lobes.

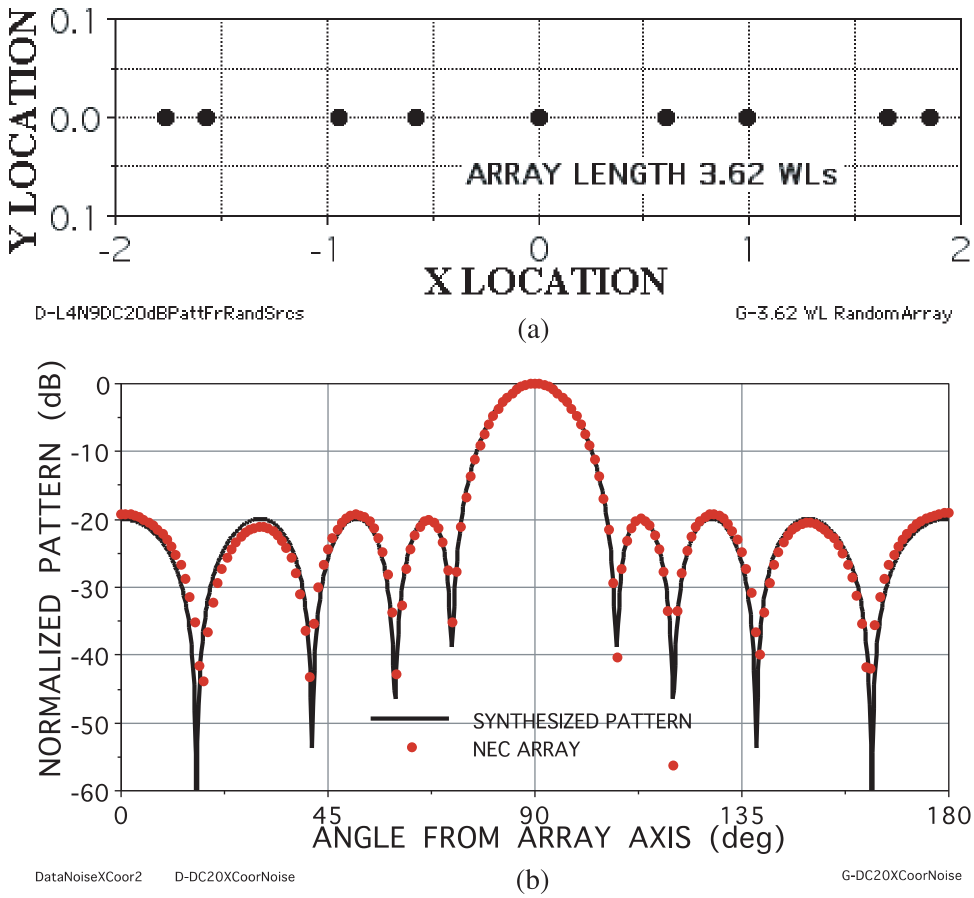

Figure 2. (a) The element locations and (b) the synthesized and NEC-computed patterns for a 9-element, 3.2-wavelength randomized array.

Table 2. Exciting Voltages and Currents for the 9-Element Dolph-Chebyshev Randomized Array Having −20 dB Sidelobes of Fig. 2.

Element No.	V Real	V Imag	I Real	I Imag
1	−5.95835E+00	−1.10614E+00	−3.34188E-02	4.61864E-06
2	−6.88189E+00	−1.99729E+00	−1.06344E-01	1.21018E-05
3	−7.32816E+00	−5.13839E+00	−1.40777E-01	9.62530E-06
4	−9.22876E+00	3.93987E+00	−1.20033E-01	5.24156E-06
5	−1.00203E+01	−1.04210E+01	−2.27637E-01	−3.97401E-07
6	−8.79976E+00	1.62886E+00	−1.32988E-01	−6.41862E-06
7	−6.49036E+00	−3.56334E+00	−1.21087E-01	−9.70153E-06
8	−6.22546E+00	−5.46955E+00	−1.29663E-01	−1.70477E-05
9	−4.57429E+00	1.18237E+00	1.19477E-02	1.97798E-06

3.3. The Non-linear Geometry Dolph-Chebyshev Array

The third example of a −20 dB DC pattern is again for a 9-element array which is 3.6 wavelengths long whose dipoles are uniformly spaced along the x-axis but displaced ±0.1 wavelengths along the y-axis

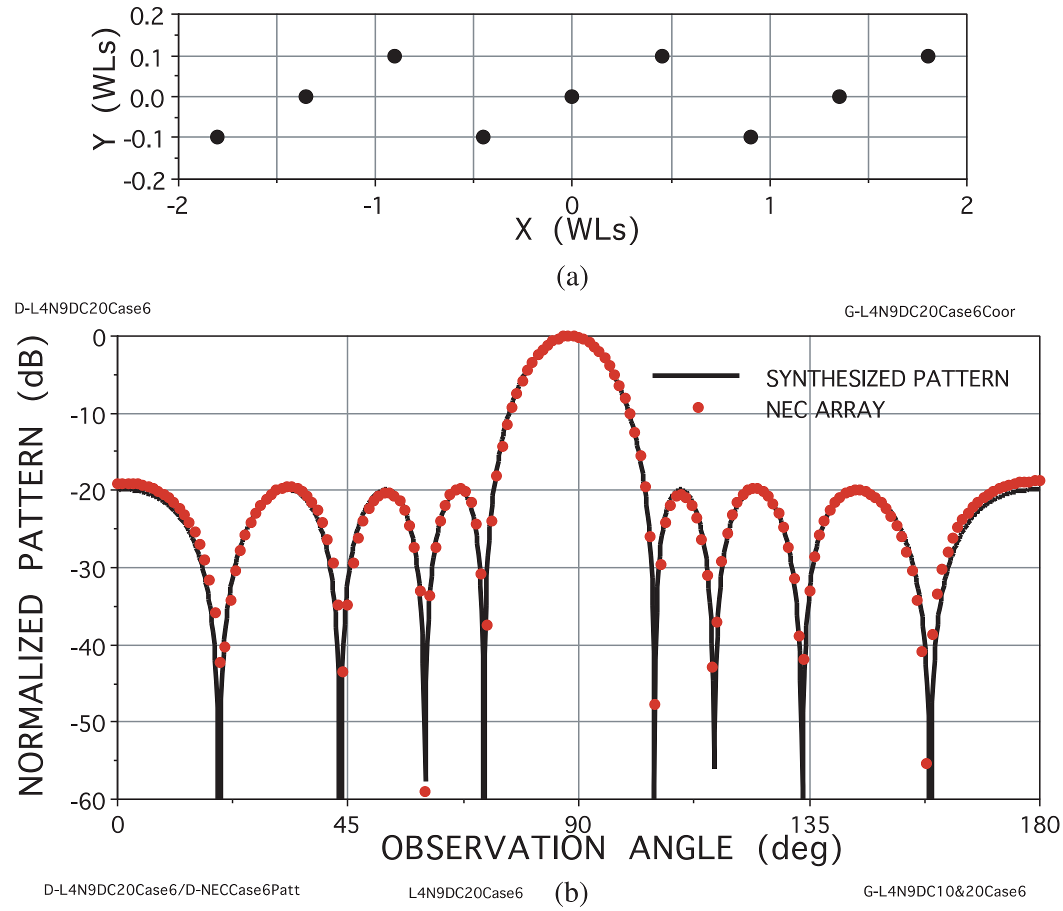

Figure 3. (a) The element locations and (b) the synthesized and NEC-computed patterns for a 9-element, 3.6-wavelength nonlinear array.

as shown in Fig. 2(a). The NEC-array match to the synthesized pattern is similar to that of Fig. 1. This array geometry is quite different from the usual linear arrangement, showing that generating a DC pattern does not require a linear array.

Table 3. Currents for 9-element Dolph-Chebyshev nonlinear array having −20 dB sidelobes of Fig. 3.

Element No.	I Real	I Imag
1	−.09279187	−.0270467
2	−.07186295	.03204793
3	−.11254131	.069066712
4	−.11436718	−.03627464
5	-.16210607	−7.684294E-26
6	−.11436718	.03627464
7	−.11254131	−.06906671
8	−.071862950	−.03204793
9	−.092791872	.027046706

3.4. The Vee-Geometry Array

The fourth example of a -20 dB DC array is a 5-wavelength long Vee-shaped array of 11 dipoles along the x-axis and successively displaced at 0.05-wavelength steps along the $-y$-axis is shown in Fig. 4. The pattern of this array does not have nulls as deep as those of Figs. 1–3 with the difference between the synthesized and NEC patterns near end fire being about 1 dB different.

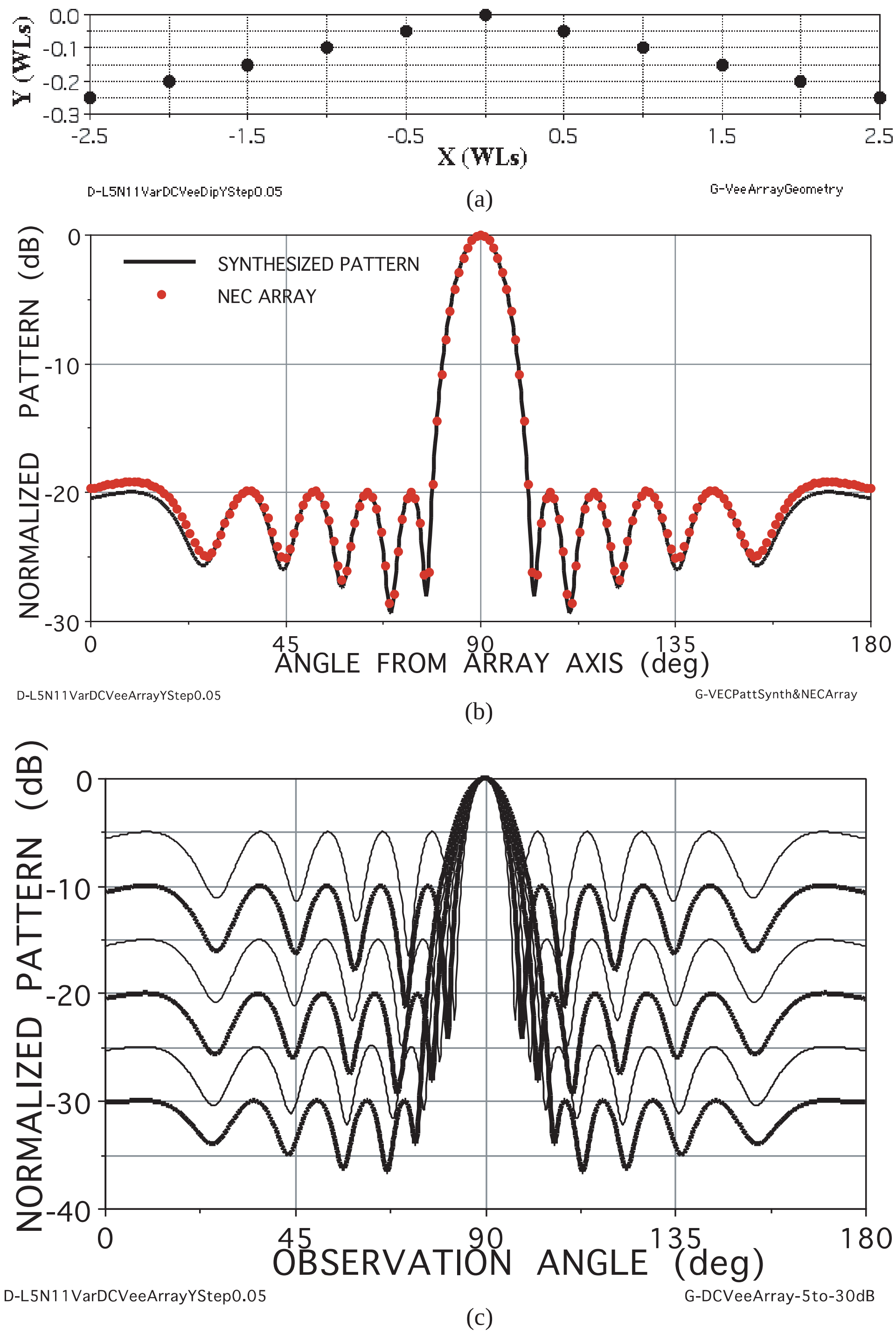

Figure 4. (a) The element locations and (b) the synthesized and NEC-computed -20 dB patterns and (c) synthesized patterns ranging from -5 to -30 dB for an 11-element 5-wavelength Vee-shaped array.

4. A TAPERED PATTERN

A 15-element 7-wavelength array having a synthesized pattern with sidelobes tapering from −15 dB in −5 dB steps to −45 dB is presented in Fig. 5. The NEC results and the synthesized patterns agree within a few tenths of a dB throughout the 45 dB range of the pattern.

Table 4. Currents for the 11-element Vee-array Dolph-Chebyshev pattern having −20 dB sidelobes of Fig. 4.

Element No.	I Real	I Imag
1	.0178059	.0470000
2	.0138911	.0641140
3	.0541936	.0656606
4	.0858278	.0713842
5	.1191862	.0395169
6	.1315947	.0167981
7	.1191862	.0395169
8	.0858278	.0713842
9	.0541936	.0656606
10	.0138910	.0641140
11	.0178059	.0470000

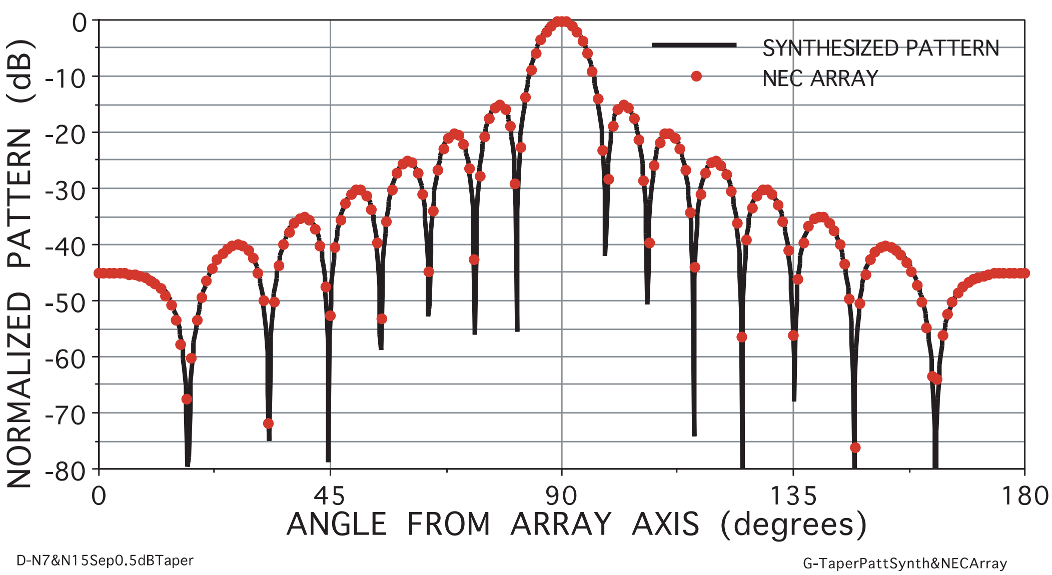

Figure 5. The synthesized and NEC tapered patterns for a 15-element, 7-wavelength array.

5. AN ALTERNATING LOBE ARRAY

An array of 15 dipoles that produce an alternating lobe pattern of −20 and −40 dBs is illustrated in Fig. 6. The agreement between the synthesized pattern and the NEC array is again within a few tenths of a dB.

Table 5. Currents for 15-element 7-wavelength array that radiates the symmetric tapered pattern of Fig. 5.

Element No.	I Real	I Imag
1	.0314320	−2.52774E−04
2	.0630510	−4.34806E−04
3	.0702429	−4.04356E−04
4	.0714669	−3.28602E−04
5	.0729315	−2.48783E−04
6	.0752856	−1.65582E−04
7	.0767993	−8.15574E−05
8	.0775808	6.10516E−24
9	.0767993	8.15574E-05
10	.0752856	1.65582E−04
11	.0729315	2.48783E−04
12	.0714669	3.28602E−04
13	.0702429	4.04356E−04
14	.0630510	4.34806E−04
15	.0314320	2.52774E−04

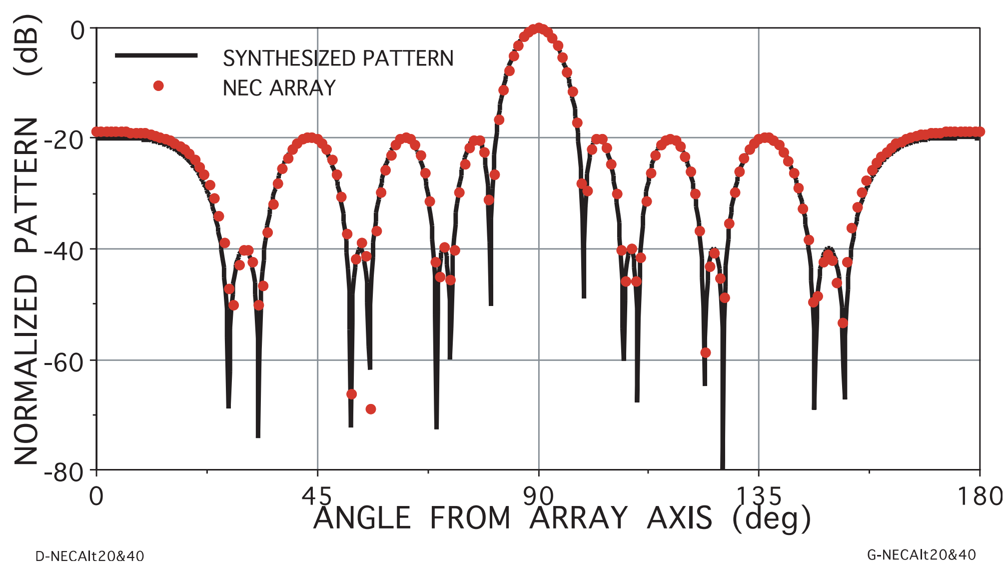

Figure 6. The synthesized and NEC alternating-lobe patterns for a 15-element, 7-wavelength array.

6. A RAMPED-PATTERN ARRAY

A synthesized, ramped pattern having a dynamic range of 70 dB with 15 lobes in 5 dB steps and its NEC counterpart is illustrated in Fig. 7. The lower 3 lobes exhibit differences as large as 5 dB but the agreement over the upper 50 dB of the patterns is graphically indistinguishable, even to the −70 dB minimum at 180 degrees. It's not clear why the NEC result differs this much from the target pattern but seems likely due to the compute precision.

Table 6. Currents for 15-element 7-wavelength array that produces the alternating-lobe pattern of Fig. 6.

Element No.	I Real	I Imag
1	.0438904	−7.42780E−04
2	.0396625	−5.65045E−04
3	.0537312	−6.34156E−04
4	.0677421	−6.40609E−04
5	.0803945	−5.79658E−04
6	.0904791	−4.27731E−04
7	.0969836	−2.28195E−04
8	.0542323	1.16675E−23
9	.0969836	2.28195E−04
10	.0904791	4.27731E−04
11	.0803945	5.79658E−04
12	.0677421	6.40609E−04
13	.0537312	6.34156E−04
14	.0396625	5.65045E−04
15	.0438904	7.42780E−04

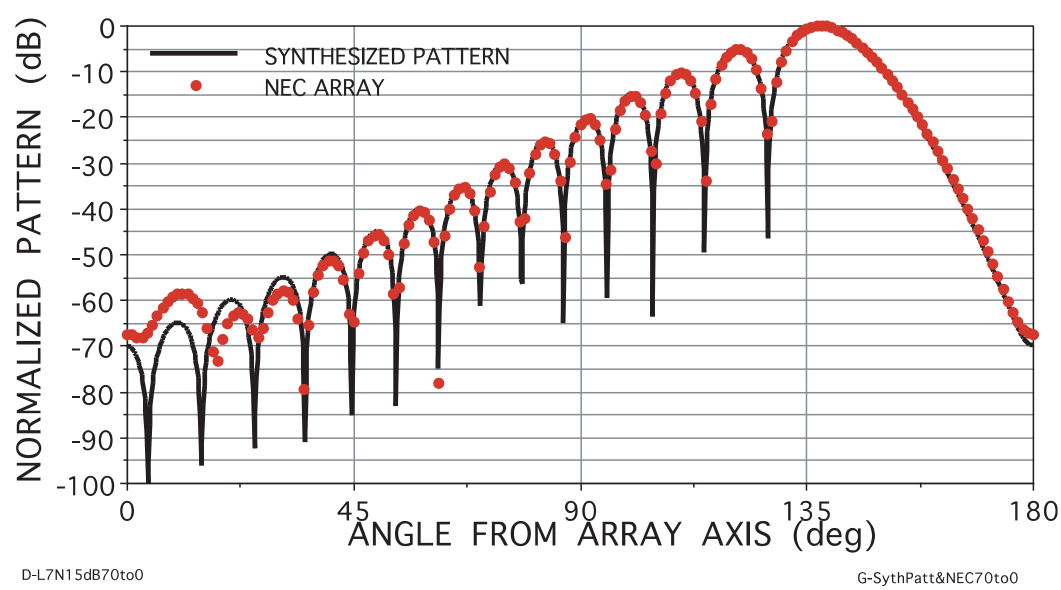

Figure 7. The synthesized and NEC ramped patterns for a 15-element, 7-wavelength array.

7. TWO-LEVEL SIDELOBE ARRAY

Another 17-element, 8-wavelength array is demonstrated in Fig. 8 for −20 and −40 dB left and right sidelobe levels. The NEC pattern agrees with the target result within a few tenths of a dB except for an approximate +2.5 dB error in both end-fire directions.

Table 7. Currents for 15-element 7-wavelength array that radiates the ramped pattern of Fig. 7.

Element No.	I Real	I Imag
1	1.43891E−02	−2.53967E−02
2	−5.10131E−02	−5.33530E−02
3	−6.11367E−02	7.20386E−02
4	9.04855E−02	2.41335E−02
5	−3.50013E−02	−7.84976E−02
6	−2.46251E−02	7.45970E−02
7	6.06884E−02	−4.19274E−02
8	−7.21317E−02	0.00000E+00
9	6.06884E−02	4.19274E−02
10	−2.46251E−02	−7.45970E−02
11	−3.50013E−02	7.84976E−02
12	9.04855E−02	−2.41335E−02
13	−6.11367E−02	−7.20386E−02
14	−5.10131E−02	5.33530E−02
15	1.43891E−02	2.53967E−02

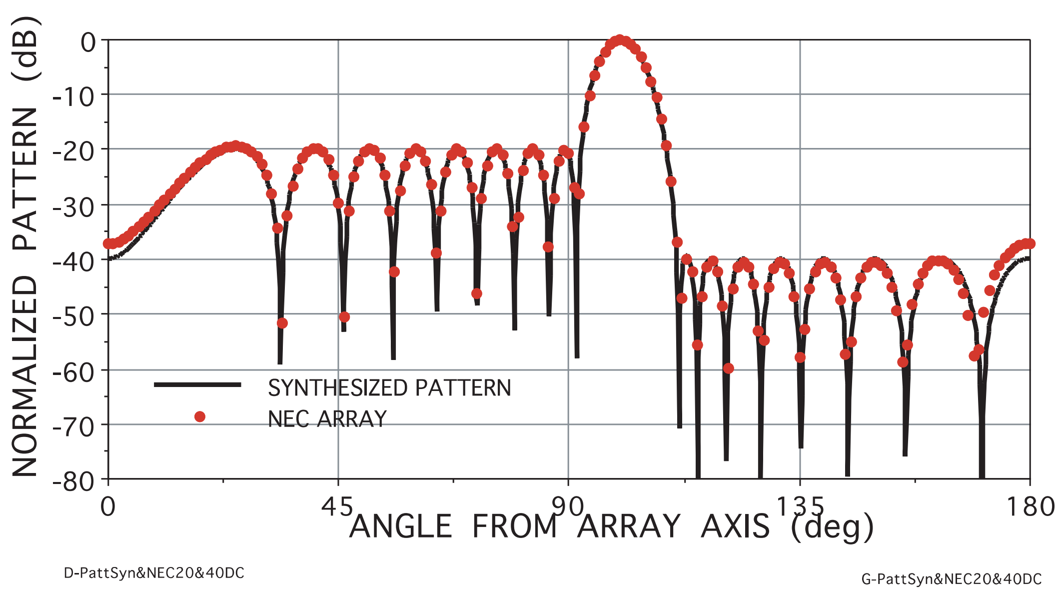

Figure 8. The synthesized and NEC patterns for a 17-element, 8-wavelength 2-level-type DC array.

8. THE TWO MAIN-LOBE ARRAY

The synthesized and NEC patterns of a 15-element, 7-wavelength array having two main lobes and −40 dB sidelobes are illustrated in Fig. 9. There is again on the order of a few tenths maximum difference between the two results. The main lobes in the example are relatively wide, a feature that might be reduced by using an array with nonuniformly spaced elements.

Table 8. Currents for 17-element 8-wavelength array that radiates the two-level-type dc pattern of Fig. 8.

Element No.	I Real	I Imag
1	2.9735e−2	1.48663e−2
2	2.51053e−2	3.87608e−2
3	3.42868e−2	5.83771e−3
4	5.429e−2	−1.19063e−2
5	3.735e−2	−4.91706e−2
6	1.4209e−2	−7.0772e−2
7	−3.62175e−2	−7.37937e−2
8	−6.8423e−2	−4.60163e−2
9	−8.99515e−2	0e+0
10	−6.8423e−2	4.60163e−2
11	−3.62175e−2	7.37937e−2
12	1.4209e−2	7.0772e−2
13	3.735e−2	4.91706e−2
14	5.429e−2	1.19063e−2
15	3.42868e−2	−5.83771e−3
16	2.51053e−2	−3.87608e−2
17	2.9735e−2	−1.48663e−2

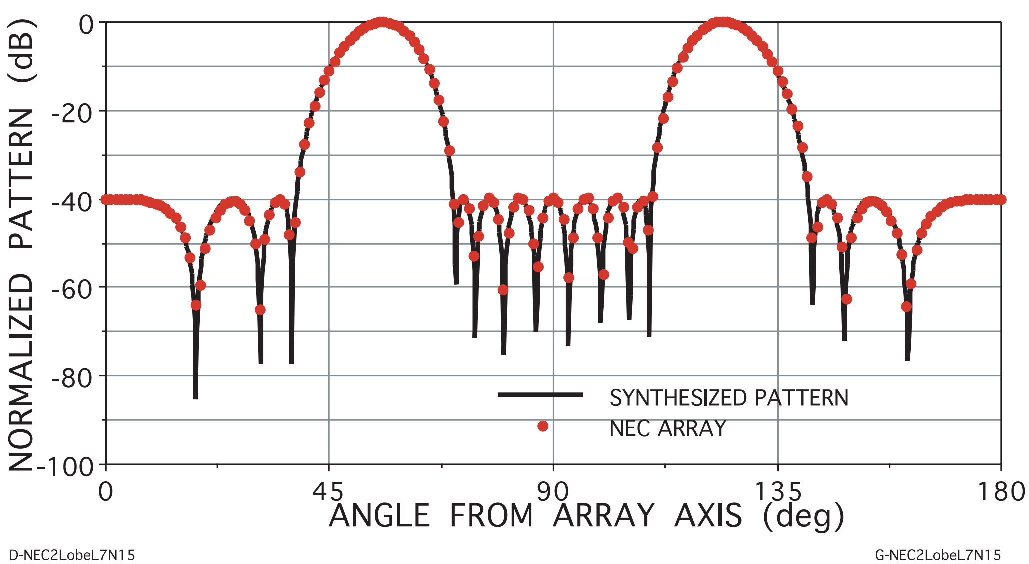

Figure 9. The synthesized and NEC two-beam DC patterns for a 15-element, 7-wavelength array.

9. SCANNED MAIN LOBE OF A DC ARRAY

A DC array, having equal-level sidelobes, is well suited for angle scanning of its main beam. An example of this possibility is shown in Fig. 10. A 17-element, 8-wavelength array with −20 dB sidelobes was synthesized with the main beam scanned to the 6'th lobe position from the center using the approach

Table 9. Currents for 15-element 7-wavelength array that radiates the two-beam-type DC pattern of Fig. 9.

Element No.	I Real	I Imag
1	3.12939E−02	−5.34272E−04
2	−2.10927E−02	3.08985E−04
3	−7.54694E−02	9.19119E−04
4	8.91787E−02	−8.75262E−04
5	9.13544E−02	−6.70290E−04
6	−1.79067E−01	8.80241E−04
7	−4.21789E−02	1.03891E−04
8	2.21963E−01	0.00000E+00
9	−4.21789E−02	−1.03891E−04
10	−1.79067E−01	−8.80241E−04
11	9.13544E−02	6.70290E−04
12	8.91787E−02	8.75262E−04
13	−7.54694E−02	−9.19119E−04
14	−2.10927E−02	−3.08985E−04
15	3.12939E−02	5.34272E−04

Table 10. Currents for 17-element 8-wavelength array for one scan angle for the DC pattern of Fig. 10.

Element No.	I Real	I Imag
1	−.0539317	−.0381817
2	.0350317	−8.80232E−03
3	−.0196925	.0395528
4	−.0202375	−.0477967
5	.0561397	.0178807
6	−.0551144	.0341402
7	.0106420	−.0685240
8	.0469328	.0547769
9	−.0730901	1.85599E−24
10	.0469328	−.0547769
11	.0106420	.0685240
12	−.0551144	−.0341402
13	.0561397	−.0178807
14	−.0202375	.0477967
15	−.0196925	−.0395528
16	.0350317	8.80232E−03
17	−.0539317	.0381817

Table 11. Real currents for a 9-element 4-wavelength array that radiates a −20 dB DC pattern and those for the $P = 2$, 3, and 4 patterns of Fig. 11.

Element No.	$P = 1$	$P = 2$	$P = 3$	$P = 4$
1	.500000	.250000	.125000	.0624999
2	.511550	.511550	.383662	.255775
3	.675150	.936833	.8988876	.730110
4	.790000	1.48074	1.76248	1.69915
5	.831350	2.09542	3.04966	3.44528
6	.789999	2.70729	4.78821	6.31920
7	.675149	3.23007	6.93649	10.7861
8	.511549	3.58256	9.37219	17.4791
9	.499999	3.87436	12.0227	27.1054
10		3.58256	14.3880	39.8125
11		3.23007	16.3597	55.1984
12		2.70729	17.6512	72.0278
13		2.09542	18.1002	88.4041
14		1.48074	17.6512	102.126
15		.936833	16.3597	109.961
16		.511549	14.3880	−2.87387E−26
17		.249999	12.0227	−4.19929E−09
18			9.37219	48.9678
19			6.93649	109.961
20			4.78821	102.126
21			3.04966	88.4041
22			1.76248	72.0278
23			.898887	55.1984
24			.383662	39.8125
25			.124999	27.1054
26				17.4791
27				10.7861
28				6.31920
29				3.44528
30				1.69915
31				.730110
32				.255775
33				.0625000

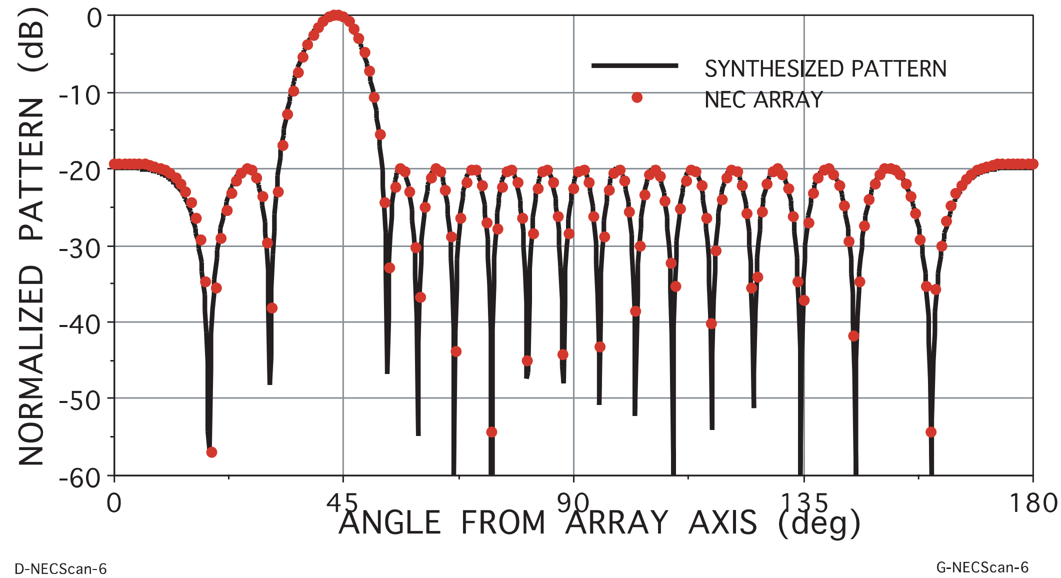

Figure 10. The synthesized and NEC −20 dB DC scanned patterns for a 17-element, 8-wavelength array.

described in [20]. Each of the 17 total lobes of the 17-element array can be made the main lobe to scan the pattern to 17 "look" angles. The NEC samples of this example match the synthesized pattern to the same degree of accuracy as found for most of the previous examples.

10. EXPONENTIATED DOLPH-CHEBYSHEV ARRAY

A last comparison of synthesized- and NEC-array patterns is presented in Fig. 11. The "$P = 1$" pattern is the standard 9-element, 4-wavelength DC −20 dB result previously shown in Fig. 1. The patterns labeled "$P = 2$" and "$P = 3$" come from squaring and cubing the $P = 1$ pattern thus creating sidelobes

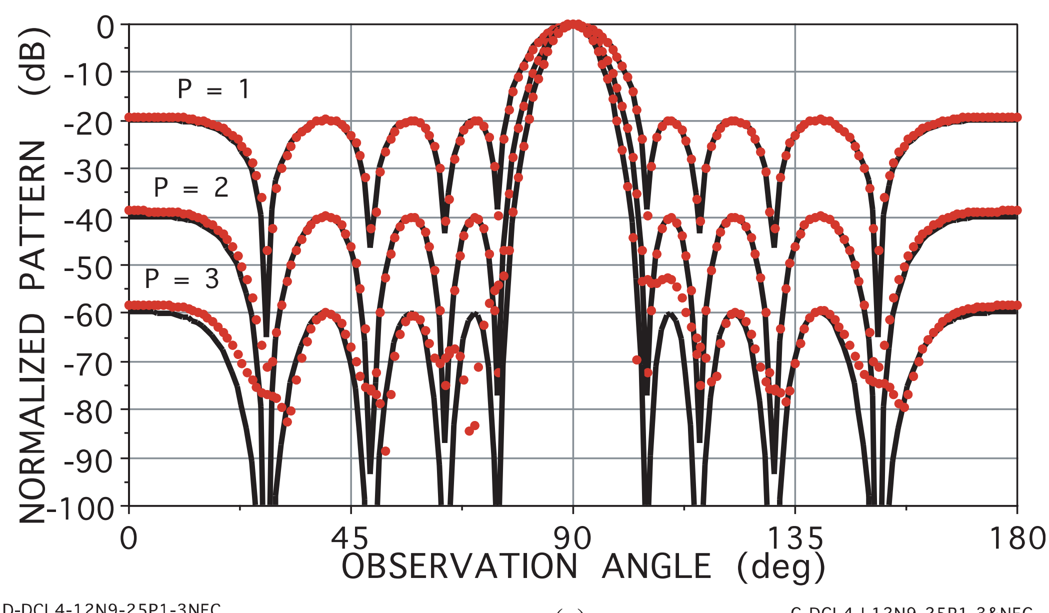

(a)

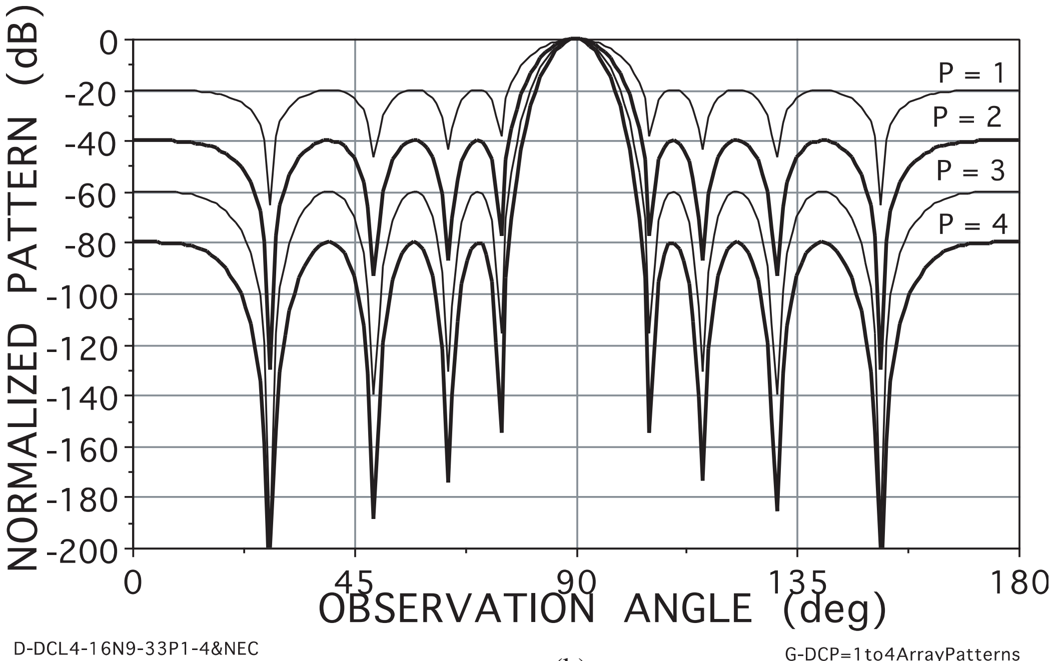

(b)

Figure 11. (a) The synthesized and NEC −20 dB DC-type patterns for a 9-element, 4-wavelength array for $P = 1$ and the $P = 2$ and $P = 3$ versions of that pattern and (b) synthesized versions for patterns with P ranging from 1 to 4.

of −40 dB and −60 dB. How these two patterns are synthesized is described in [3]. Prony-Method synthesis yields arrays 8 and 12 wavelengths long having 17 elements and 25 elements, respectively. The standard DC arrays of 8 and 12 wavelengths would have 17 and 25 lobes. The number of lobes in the $P = 2$ and $P = 3$ versions retain the 9-lobe structure of the 4-wavelength array. However, the widths of the lobes are successively reduced and their null depths are increased. The NEC pattern for $P = 3$ differs substantially from the synthesized version, likely due to inadequate compute precision, while the agreement demonstrated with the other two patterns is similar to the other NEC results.

11. SUMMARY

The output of the typical pattern-synthesis exercise is normally the individual currents needed to produce a desired radiation pattern from a specified array geometry. The array is typically comprised of radiating elements, such as dipole antennas, that are spaced closely enough that mutual interactions between them needs to be taken into account. Whether that pattern can be produced by a physical array requires the further step of determining the exciting voltages needed to produce the desired individual currents. The goal of this discussion has been to explore the latter step for a variety of antenna patterns using the NEC computer model. For reference purposes the NEC voltages needed to match the target pattern were given for two cases in Tables 1 and 2 and the array element currents were included in Tables 1–11 for all of the synthesized patterns.

The NEC results were generally found to agree within a few 10'ths of a dB for the patterns for which they were developed. The two exceptions where the differences were greater occurred when the lobe maxima were at levels below −50 dB. The final step in demonstrating the practicality of producing a desired synthesized pattern would be implementation and testing an array design in actual hardware, a step beyond this study.

REFERENCES

1. Schelkunoff, S. A., "A mathematical theory of linear arrays," *Bell System Technical Journal*, Vol. 22, 80–107, 1943.
2. Dolph, C. L., "A current distribution for broadside arrays which optimizes the relationship between beam width and side-lobe level," *Proceedings of the IRE*, Vol. 34, No. 7, 335–348, 1946.
3. Woodward, P. M., "A method of calculating the field over a plane aperture required to produce a given polar diagram," *Journal Institute of Electrical Engineering*, Pt. IIIA, Vol. 93, 1554–1558, 1946.
4. Taylor, T. T., "Design of line-source antennas for narrow beamwidth and low sidelobes," *IRE Transactions on Antennas and Propagation*, Vol. 7, 16–28, 1955.
5. Elliott, R. S., "On discretizing continuous aperture distributions," *IEEE Transactions on Antennas and Propagation*, Vol. 25, No. 5, 617–621, September 1977.
6. Elliott, R. S., *Antenna Theory and Design*, Prentice-Hall, Englewood Cliffs, NJ, 1981.
7. Balanis, C. A., *Antenna Theory: Analysis and Design*, Harper & Row, Publishers, New York, 1982.
8. Kummer, W. H., "Basic array theory," *Proceedings of the IEEE*, Vol. 80, No. 1, 127–140, January 1992.
9. Chang, H.-P., T. K. Sarkar, and O. M. C. Pereira-Filho, "Antenna pattern synthesis utilizing spherical bessel functions," *IEEE Transactions on Antennas and Propagation*, Vol. 48, No. 6, 853–859, June 2000.
10. Durr, M., A. Trastoy, and F. Ares, "Multiple-pattern linear antenna arrays with single prefixed amplitude distributions: Modified Woodward-Lawson synthesis," *Electronics Letters*, Vol. 36, No. 16, 1345–1346, 2000.
11. Marcano, D. and F. Duran, "Synthesis of antenna arrays using genetic algorithms," *IEEE Antennas and Propagation Magazine*, Vol. 42, No. 3, 12–20, June 2000.
12. Virga, K. L. and M. L. Taylor, "Transmit patterns for active linear arrays with peak amplitude and radiated voltage distribution constraints," *IEEE Transactions on Antennas and Propagation*, Vol. 49, No. 5, 732–730, May 2001.
13. Bucci, O. M., M. D'Urso, and T. Isernia, "Optimal synthesis of difference patterns subject to arbitrary sidelobe bounds by using arbitrary array antennas," *IEE Proceedings on Microwaves, Antennas and Propagation*, Vol. 152, No. 3, 129–137, 2005.
14. Vescovo, R., "Consistency of constraints on nulls and on dynamic range ratio in pattern synthesis for antenna arrays," *IEEE Transactions on Antennas and Propagation*, Vol. 55, No. 10, 2662–2670, October 2007.
15. Liu, Y., Z. Nie, and Q. H. Liu, "Reducing the number of elements in a linear antenna array by the matrix pencil method," *IEEE Transactions on Antennas and Propagation*, Vol. 56, No. 9, 2955–2962, September 2008.
16. Gomez, N. G., J. J. Rodriguez, K. L. Melde, and K. M. McNeill, "Design of low-sidelobe linear arrays with high aperture efficiency and interference nulls," *IEEE Antennas and Wireless Propagation Letters*, Vol. 8, 607–610, 2009.
17. Comisso, M. and R. Vescovo, "Fast iterative method of power synthesis for antenna arrays," *IEEE Transactions on Antennas and Propagation*, Vol. 57, No. 7, 1952–1962, July 2009.
18. Wong, A. M. H. and G. V. Eleftheriades, "Adaptation of Schelkunoff's superdirective antenna theory for the realization of superoscillatory antenna arrays," *IEEE Antennas and Wireless Propagation Letters*, Vol. 9, 315–318, 2010.
19. Apostolov, P. S., "Linear equidistant antenna array with improved selectivity," *IEEE Transactions on Antennas and Propagation*, Vol. 59, No. 10, 3940–3943, October 2011.
20. Zhang, T. and W. Ser, "Robust beampattern synthesis for antenna arrays with mutual coupling effect," *IEEE Transactions on Antennas and Propagation*, Vol. 59, No. 8, 2889–2895, 2011.
21. Singh, H., H. L. Sneha, and R. M. Jha, "Mutual coupling in phased arrays: A review," *International Journal of Antennas and Propagation*, 23 pages, 2013.

22. Miller, E. K., "Synthesizing linear-array patterns via matrix computation of element currents," *IEEE Antennas and Propagation Society Magazine*, Vol. 55, No. 5, 85–96, October 2013.
23. Miller, E. K., "Using Prony's Method to synthesize discrete arrays for prescribed source distributions and exponentiated patterns," *IEEE Antennas and Propagation Society Magazine*, Vol. 57, No. 1, 147–163, February 2015.